8th International Tribology Conference
Osma internacionalna konferencija o tribologiji
Beograd, 8. - 10. oktobra 2003.

ROLE OF TOOTH STIFFNESS IN LUBRICATION CHARACTERISTICS OF WORM GEARING

A. H. ELKHOLY, A. H. FALAH and **E. M. ALAWADI**,
Mechanical Engineering Department, Kuwait University, Kuwait

S u m m a r y

An approach has been developed by the authors to estimate the tooth stiffness variation of worm gear drives, and to calculate the instantaneous tooth meshing stiffness. In the approach, a closed form solution that is substantiated by a finite element (FE) modeling based on the exact tooth geometry, which ensures that the worm gear teeth are in localized contact is presented. The geometric modeling method for involute worm gears allows the tooth elastic deformation of worm gear drives under different load conditions to be investigated. On the basis of both the closed form and finite element analysis, the instantaneous meshing stiffness and combined stiffness of worm and gear are predicted. In comparison with existing methods, this approach provides more accurate tooth geometry and stiffness variation that can be extended to calculate load capacity rating, lubrication characteristics and relevant stresses of worm gear drives.

Keywords: *worm gears, localized tooth contact, lubrication, tooth stiffness*

1. INTRODUCTION

Worm gears have been widely used in industry for many years because they achieve high reduction ratios, low speed and low noise operation. In the case of conventional design, gear specifications are determined using a standardized method. However, small size worm gears that are used for transmitting high power are expected to wear at an accelerated rate raising the problem of failure of the teeth due to fatigue. Therefore, development of a method of rational design for such teeth is desired. If load distribution of gears along the contact line is determined, oil film thickness , contact pressure and tooth root stress at an arbitrary position on the tooth surface can be calculated.

However, the accurate calculation of tooth load distribution requires accurate determination of stiffness variation of meshing teeth from beginning to end of contact.

Yang et al [1] used a 3-D Finite Element Analysis to determine load sharing and stiffness variation of contacting worm drive. Their analysis produced reliable results, but it took too much computing time. Zhang et al [2], on the other hand, used Finite Element Analysis, as well to determine loads and stresses. But the computation time was a major drawback in their analysis. Therefore, we plan to develop a calculation method to determine tooth stiffness using tooth deflection equations and substantiate the results by Finite Element Analysis (FEA). The calculated results ought to be compared with experimental results obtained from literature in order to gain recognition.

2. MESH GEOMETRY:

The cylindrical (single enveloping) worm and gear of a set have the same hand of helix. The lead angle λ on the worm equals the helix angle ψ on the gear and the worm axial pitch p_x and the gear transverse circular pitch p_t are equal as well

for a 90° shaft angle. The worm lead angle is the complement of the worm helix angle. The pitch radius of the gear R_2 is the radius measured on a plane containing the worm axis and is determined from:

$$R_2 = \frac{N_G \ p_t}{2\pi} \tag{1}$$

where N_G is the number of teeth on the gear. The Lead of worm L is calculated from:

$$L = \frac{p_t \cos\phi}{\cos\lambda}$$

where ϕ is the pitch pressure angle. The center distance of the gear set C is related to the root R_r, pitch R and outside R_o radii of the worm and gear as follows:

$$\begin{aligned} C &= R_1 + R_2 \\ &= R_{r_1} + R_{o_2} \\ &= R_{o_1} + R_{r_2} \end{aligned} \tag{2}$$

where 1, 2 refer to the worm and gear, respectively. Note that the tooth clearance is neglected in driving equation (2).

The worm base radius is calculated from:

$$R_{b_1} = \frac{L}{2\pi \tan\lambda} \tag{3}$$

whereas the worm form radius R_f (radius to top of fillet on worm thread) is determined from [3].

$$\begin{aligned} R_f = \mathrm{SQRT}\{&(R_{r_1} + R_{o_2})^2 + R_{o_2}^2 \\ &- 2[R_{o_2}(R_{r_1} + R_{o_2})]\cos\delta\} \end{aligned} \tag{4}$$

where δ is determined from:

$$\delta = \sin^{-1}\left[\frac{R_{b_1}}{R_{r_1} + R_{o_2}}\right] \tag{5}$$

The actual contact ratio CR of the worm gear set is calculated from:

$$\begin{aligned} CR = \alpha \Big[&\sqrt{R_{o_2}^2 - R_{b_2}^2} \\ &- R_2 \cos\phi \tan\lambda \\ &+ \frac{\sqrt{R_{o_1}^2 - R_{b_1}^2} - R_1}{\sin\lambda}\Big] \end{aligned} \tag{6}$$

where R_{b_2} is the base radius of the gear and is determined from

$$R_{b_2} = R_2 \cos\phi \tag{7}$$

and $\alpha = \dfrac{1}{L \ \mathrm{Cos}\lambda}$

The contact ratio, given in (6), is the number of teeth on the worm and gear that are in simultaneous mesh at a given instant.

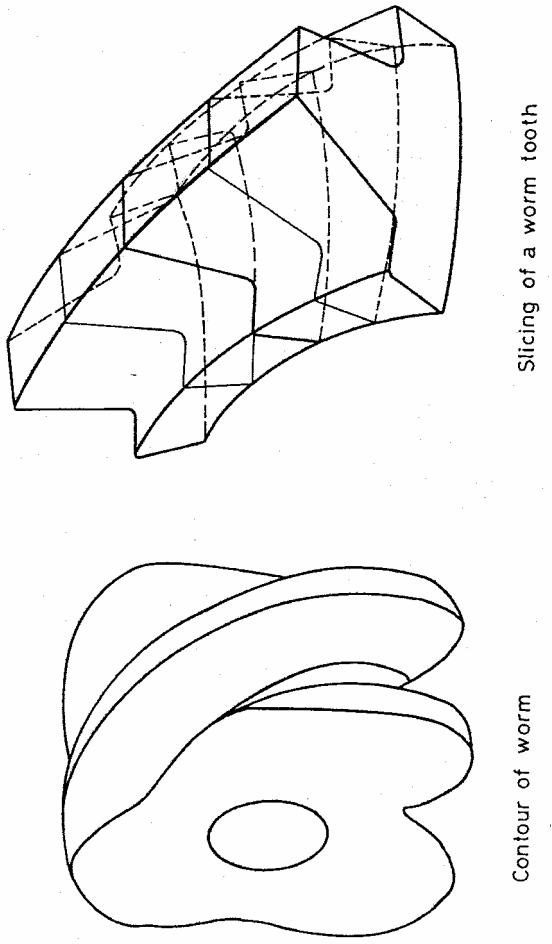

Figure 1. Worm model

3. GEAR MESH MODELING:

To facilitate the analysis and use the experience already established in literature, both the worm and gear were modeled as a series of spur gear segments (slices) whose orientation depends on their location within the mesh. This approach was first introduced by Tredgold [4] and later used to model non-spur gears. Figure (1) and Figure (2) show the modeling of the worm and gear, respectively, while Figure (3) shows the slicing directions of the set as well as the various contact lines that take place along the tooth flank

from start to end meshing. The exact number of contact lines that takes place at a given instant of time is determined by the magnitude of the contact ratio. Each slice on the set can be modelled as a spur gear if the width of the slice is made relatively small. Therefore, the accuracy of results will depend on the number of the slices that represent both the worm and the gear. The more these slices, the better the results that are obtained. Moreover, spur gear slices on the worm will have the same root and outside diameters as the worm itself, but their exact points of contact with their counterpart slices of the gear will depend on their location. On the other hand, the geometry of the slices on the gear will have variable root and outside diameters depending on their location as shown in Figure (3). The face width of each slice of the set depends also on the geometry and the number of slices considered.

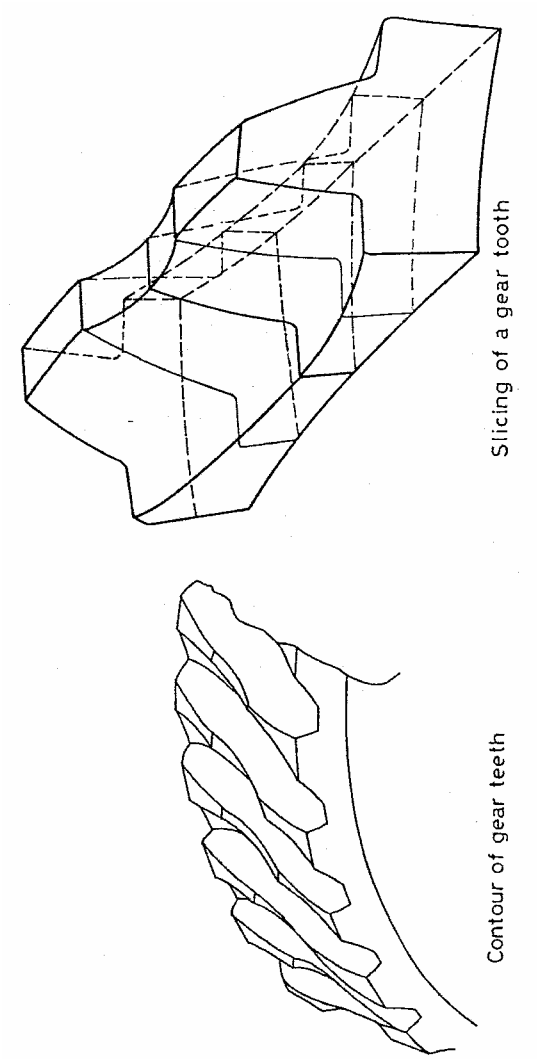

Figure 2. Gear Model

4. SLICE DEFLECTION AND STIFFNESS CALCULATION:

Each slice on either the worm or gear is considered as a straight spur gear whose main dimensions depend upon the location of the slice. If a slice is subjected to a normal load F_i, then the total deflection δ is calculated from the equation given in [5] which accounts for bending, shear, Hertzian contact and foundation deformations.

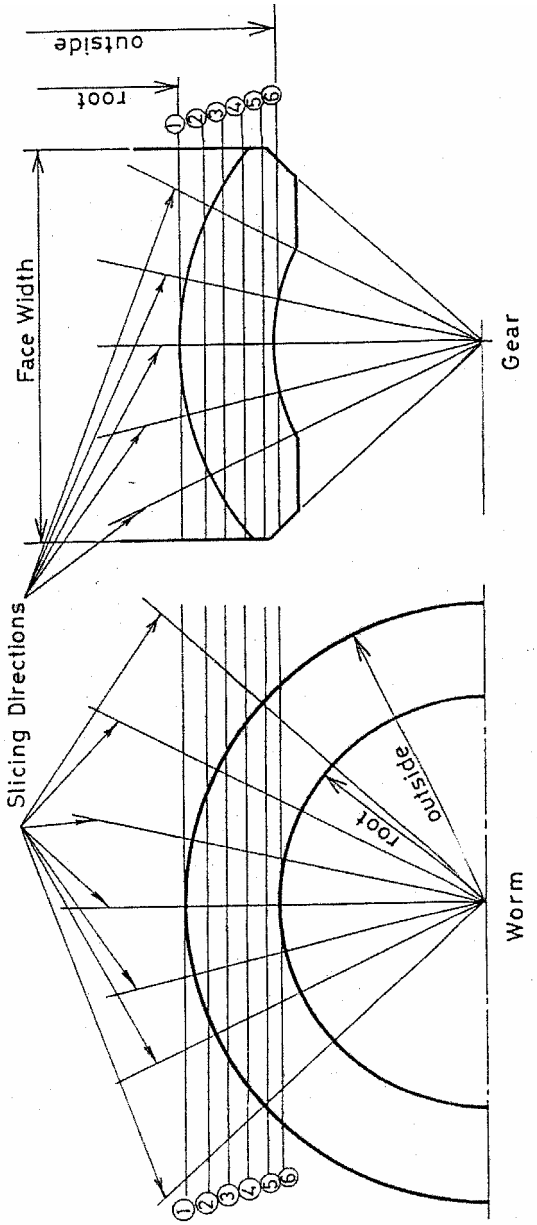

Figure 3. Geometry and Contact Lines

The slice stiffness K_i can then be expressed as

$$K_i = \frac{F_i}{\delta} \qquad i = 1, 2, ..., n \qquad (8)$$

where subscript i refers to the slice under consideration. The stiffnesses of all slices on the worm and the corresponding ones on the gear can therefore be determined.

5. FINITE ELEMENT ANALYSIS:

A displacement type finite element method is applied for the analysis of all slices that model the worm and gear derive. Curved, 8 node 2 D quadratic elements are used in each slice of the worm and gear as shown in Figure (4). The finite element grid shown in the figure was generated automatically including the element numbering, the definition of element topology, the calculation of nodal coordinates, and the specification of boundary conditions. The numbers and sizes of elements can be arbitrarily chosen in the main directions and in different regions of the worm and the gear in order to get finer mesh when required. Such a variation of the number and sizes of elements also gives the opportunity to investigate the convergency of the solution. Figure (4) shows the mapping of worm thread and gear tooth. In the calculations a much finer mesh than that presented in the figure is applied.

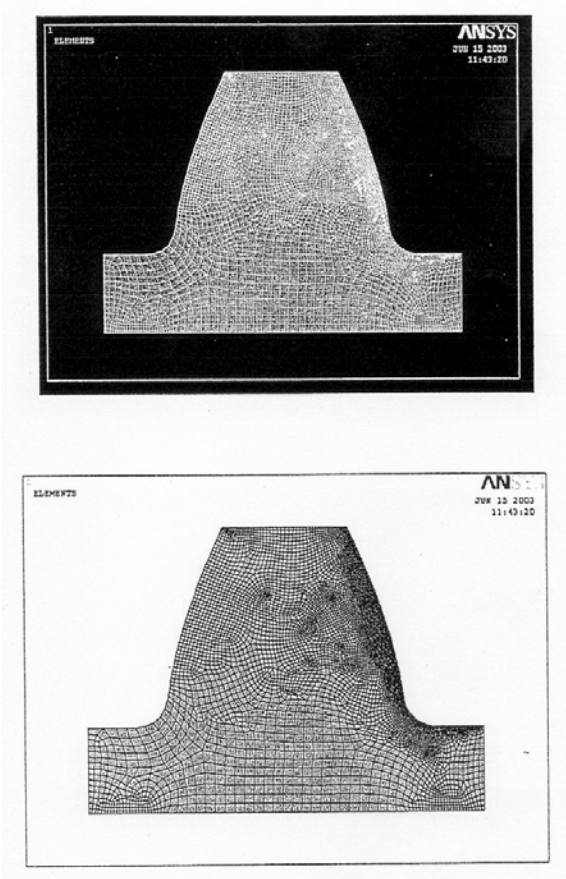

Figure 4. Finite Element Grid

The accurate geometric modeling of the tooth profile of both the worm and gear was introduced prior to the implementation of the Finite Element grid using the criteria presented in [6]. The modeling of the entire tooth was then exported as an IGES file that is a standard file format for graphic exchange. Then the IGES files are imported into the software ANSYS 6.1 [7]. When the IGES file is retrieved in ANSYS, it is usually only a geometric model with the surface information. The preprocessor of ANSYS is used to create the element type and choose the material property for the analysis.

6. RESULTS:

In this section, we demonstrate an example calculated by the program developed using closed form solution and Finite Element Analysis. Table (1) shows the dimensions of the worm gearing which was obtained from [8]. The tooth profile was not modified and is assumed free of errors. The stiffness variation along tooth flank of the worm was calculated from equation (8) and the results were compared with those obtained from FEA. The results from the closed form solution are given in Figure (5) and were found to be in good agreement with those obtained from the FEA. It was also found that there exist two teeth in simultaneous contact during part of the mesh.

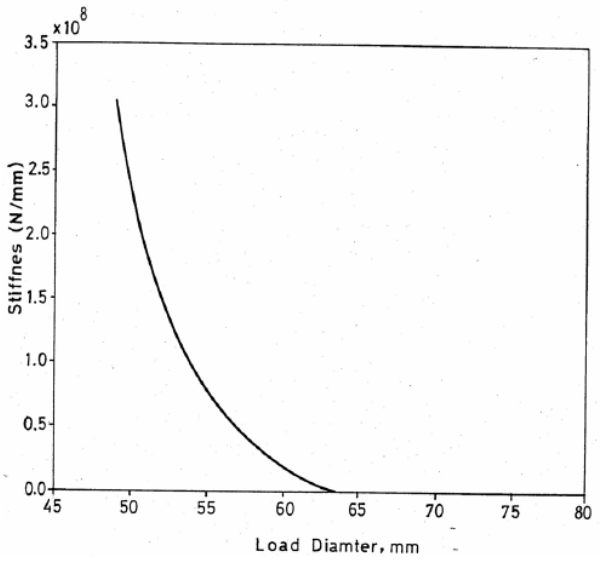

Figure 5. Stiffnes Variation

7. CONCLUSIONS:

In the present study, we have developed a program for the accurate calculation of tooth stiffness variation along tooth flank of worm gear derive. The results are to be extended for calculating load distribution and sharing among

meshing teeth. This will lead to the determination of lubrication characteristics and relevant stresses. The calculated stiffness variation was compared with that obtained from FEA.

Table 1: *Gear Specifications*

		Worm	Wheel
Module,	mm	6.2	
Pressure angle,	deg	20	
Lead angle,	deg	17.896	
Center distance,	mm	125	
Number of teeth,		3	31
Pitch circle diameter,	mm	57.6	192.4
Averaged diameter,	mm	57.8	192.2
Outside diameter,	mm	68.0	204.8
Root diameter,	mm	41.2	178.0
Face width,	mm	--	46

The results obtained are summarized as follows:

1. *Tooth stiffness of both worm and gear has a high value close to the root and decreases gradually towards the top.*
2. *Finite Element results agree very well with those obtained from the developed program.*
3. *The results from the developed program can be obtained in a very short time as compared to the time required for using FEA.*
4. *The developed program can be programmed using any computer language such as: BASIC, FOTRAN, MATLAB, C, ... etc. and the results are obtainable almost instantly.*

8. ACKNOWLEDGMENT:

The authors wish to acknowledge the Research Administration of Kuwait University for their sponsorship in supporting research.

9. REFERENCES:

[1] Yang, F., Su, D., and Gentle, C.R., "Finite Element Modeling and Load Share Analysis for Involute Worm Gears with Localized Tooth Contact", Proc. Instn Engrs, Vol. 215, part C, pp. 805-816, 2001.

[2] Zhang, J.J., Esat, I.I., and Shi, Y.H., "Load Analysis with Varying Mesh Stiffness", Computers &Structures, Vol. 70, pp. 273-280, 1999.

[3] Buckingham, E., and Ryffel, H.H., "Design of Worm & Spiral Gears", Industrial press Inc., 1981.

[4] Shigley, J.E., "Mechanical Engineering Design", 1st Metric Ed., McGraw-Hill, New York, pp. 552-557, 1987.

[5] Elkholy, A.H., "Tooth Load Sharing in High Contact Ratio Spur Gears", ASME Tran., Journal of Mechanisms, Transmissions, and Automation in Design, Vol. 107, pp. 11-16, March 1985.

[6] Elkholy, A.H., "Finite Element Grid Generation of Spur Gears", Int. J. of Computer Applications in Technology, Vol. 9, No. 2/3, pp. 159-164, 1996.

[7] ANSYS-User's Manual for Version 6.1, Vol. 1, Swanson Analysis Systems, Houston, Pennsylvania, 2002.

[8] Sudoh, K., Tanaka, Y., Matsumoto, S. and Tozaki, Y., "Load Distribution Analysis Method for Cylindrical Worm Gear Teeth", Int. J. JSME, Series C, Vol. 39, No. 3, pp., 606-613, 1996.